Caenorhabditis elegans chaperonin CCT/TRiC is required for actin and tubulin biogenesis and microvillus formation in intestinal epithelial cells

Keiko Saegusa[a,*], Miyuki Sato[b,*], Katsuya Sato[a], Junko Nakajima-Shimada[c], Akihiro Harada[d], and Ken Sato[a]

[a]Laboratory of Molecular Traffic and [b]Laboratory of Molecular Membrane Biology, Institute for Molecular and Cellular Regulation, and [c]School of Health Sciences, Gunma University, Maebashi, Gunma 371-8512, Japan; [d]Department of Cell Biology, Graduate School of Medicine, Osaka University, Suita, Osaka 565-0871, Japan

ABSTRACT **Intestinal epithelial cells have unique apical membrane structures, known as microvilli, that contain bundles of actin microfilaments. In this study, we report that *Caenorhabditis elegans* cytosolic chaperonin containing TCP-1 (CCT) is essential for proper formation of microvilli in intestinal cells. In intestinal cells of *cct-5(RNAi)* animals, a substantial amount of actin is lost from the apical area, forming large aggregates in the cytoplasm, and the apical membrane is deformed into abnormal, bubble-like structures. The length of the intestinal microvilli is decreased in these animals. However, the overall actin protein levels remain relatively unchanged when CCT is depleted. We also found that CCT depletion causes a reduction in the tubulin levels and disorganization of the microtubule network. In contrast, the stability and localization of intermediate filament protein IFB-2, which forms a dense filamentous network underneath the apical surface, appears to be superficially normal in CCT-deficient cells, suggesting substrate specificity of CCT in the folding of filamentous cytoskeletons in vivo. Our findings demonstrate physiological functions of CCT in epithelial cell morphogenesis using whole animals.**

Monitoring Editor
Jeffrey D. Hardin
University of Wisconsin

Received: Sep 16, 2013
Revised: Jul 29, 2014
Accepted: Aug 6, 2014

INTRODUCTION

The plasma membrane of most epithelial cells in animals is separated into apical and basolateral membranes by cell–cell junctions (Rodriguez-Boulan *et al.*, 2005). The apical surface of intestinal epithelial cells contains characteristic membrane structures known as microvilli. These structures are plasma membrane protrusions containing tightly bundled actin microfilaments. Microvilli expand the cell surface area of the apical region and are believed to support efficient nutrient absorption or filtration. Although various proteins, including actin-bundling and membrane linker proteins and specific lipids, have been identified as key molecules for establishment of the microvillus brush border, our understanding of the molecular mechanisms underlying microvillus formation in vivo is still limited (Nambiar *et al.*, 2010; Gloerich *et al.*, 2012; Ikenouchi *et al.*, 2013).

Caenorhabditis elegans is a useful model for studying the mechanism(s) of the formation and maintenance of polarized epithelial cells. In *C. elegans*, the intestine forms a simple tube made up of 20 polarized cells, with apical (lumenal) and basolateral membranes (McGhee, 2007; McGhee *et al.*, 2009). The apical membranes of worm intestinal cells form a number of microvilli similar to those observed in mammalian epithelial cells. The cytoskeleton, comprising microfilaments, microtubules, and intermediate filaments, plays an essential role in the formation and maintenance of the epithelial cell structure. Of the five actin genes in the *C. elegans* genome, *act-5* is specifically expressed in intestinal and excretory cells, whereas the other actin genes are widely expressed in many tissues (Waterston *et al.*, 1984; MacQueen *et al.*, 2005). Deletion of *act-5* results in complete loss of microvilli in the intestine and leads to lethality during the

This article was published online ahead of print in MBoC in Press (http://www.molbiolcell.org/cgi/doi/10.1091/mbc.E13-09-0530) on August 20, 2014.

*These authors contributed equally to this work.

Address correspondence to: Ken Sato (sato-ken@gunma-u.ac.jp), Akihiro Harada (aharada@acb.med.osaka-u.ac.jp).

Abbreviations used: BSA, bovine serum albumin; CCT, chaperonin containing TCP-1; ERM, ezrin, radixin, moesin; FRAP, fluorescence recovery after photobleaching; GFP, green fluorescent protein; HEPES, 4-(2-hydroxyethyl)-1-piperazineethanesulfonic acid; IPTG, isopropyl β-D-thiogalactopyranoside; mC, mCherry; PBS, phosphate-buffered saline; RNAi, RNA interference; TRiC, TCP-1 ring complex.

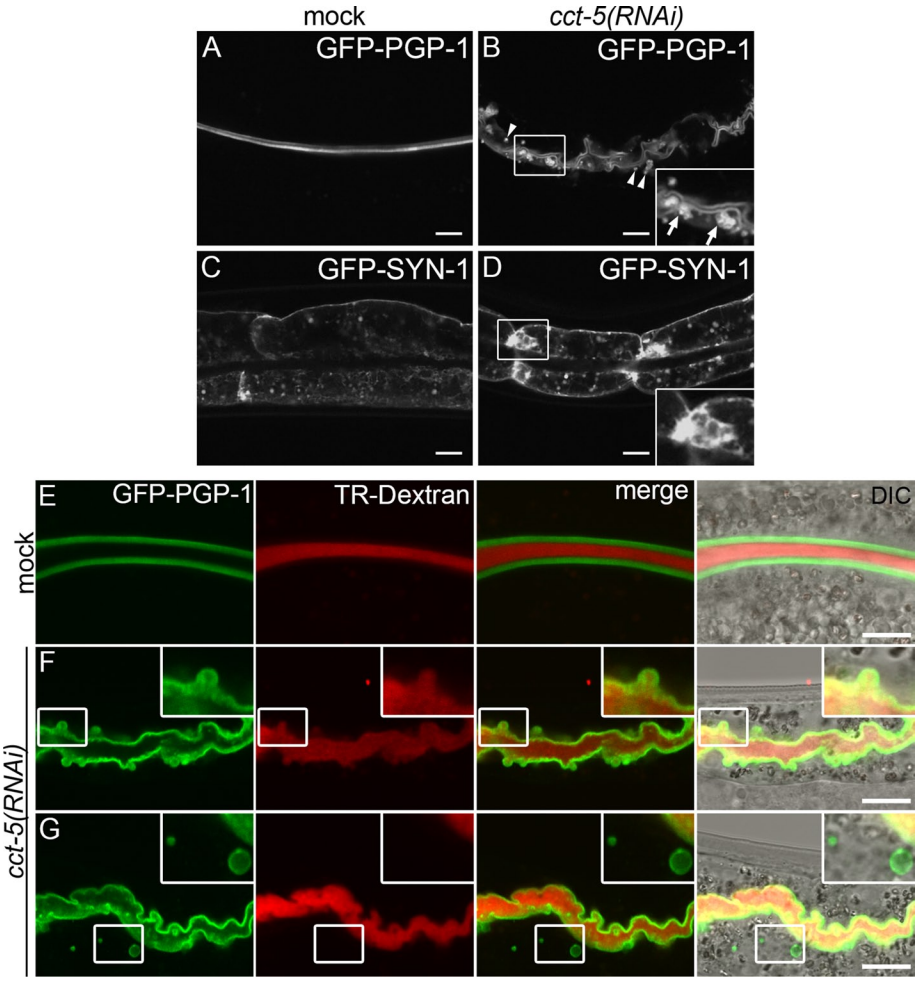

FIGURE 1: CCT-5 is required for the normal apical morphology of intestinal cells. (A–D) In the wild-type intestine, GFP-PGP-1 and GFP-SYN-1 are localized to the apical and basolateral membranes, respectively (A, C). In *cct-5(RNAi)* animals, GFP-PGP-1 is largely targeted to the apical membrane but partly localized on abnormal, bubble-like membrane structures (B, inset, arrows) and internal vesicles (B, arrowheads). GFP-SYN-1 is mainly targeted to the basolateral membrane in *cct-5(RNAi)* animals (D), whereas strong GFP signals are also observed in cytoplasmic structures proximal to the lateral membrane (D, inset). An enlarged (×2) image of the boxed area is shown in each inset (B, D). (E–G) Worms expressing GFP-PGP-1 (green) were fed with Texas Red–dextran (red) and observed by confocal microscopy. The apical bubble-like structures formed in *cct-5(RNAi)* animals are filled with Texas Red–dextran (F, insets). In addition, there are some GFP-PGP-1–labeled cytoplasmic punctate structures that do not contain Texas Red–dextran (G, insets). In all experiments, L1 larvae were treated with RNAi for 3 d. Scale bars, 10 μm.

first larval stage. These findings indicate that the ACT-5 protein is essential for microvillus formation and that microvilli are essential structures for animal viability (MacQueen *et al.*, 2005). The intermediate filaments have a long, central α-helical rod domain with heptad repeats that form a dimer (Carberry *et al.*, 2009). IFB-2 and IFC-2, which are intermediate filaments expressed in the intestine of *C. elegans*, are localized to the subapical layer of the "terminal web" and form a dense filamentous network (Bossinger *et al.*, 2004; Karabinos *et al.*, 2004; Segbert *et al.*, 2004; Carberry *et al.*, 2009). Knockdown of these intestinal intermediate filaments results in an abnormal, bubble-like morphology of the apical membrane, suggesting the importance of intermediate filaments in maintaining the apical membrane structure of intestinal tubes (Bossinger *et al.*, 2004; Hüsken *et al.*, 2008). Microtubules play an essential role in polarization of the intestinal primordium, although their specific functions in differentiated intestinal cells are not well understood in *C. elegans*. In intestinal primordial cells that are beginning to polarize, microtubules are concentrated near the apical surface, extend along the lateral surface, and to a lesser extent localize to the basal region (Leung *et al.*, 1999; Feldman and Priess, 2012). Inhibition of microtubule formation causes a delay in nuclear migration to the apical surface and cytoplasmic polarization (Leung *et al.*, 1999). Several genes, including ERM-1 and IFO-1, have been identified to regulate apical morphogenesis in the intestinal cells of *C. elegans* (Gobel *et al.*, 2004; Carberry *et al.*, 2012).

The folding of cytoskeletal components is largely dependent upon the eukaryotic cytosolic chaperonin containing TCP-1 (CCT), which is also known as the TCP-1 ring complex (TRiC; Horwich *et al.*, 2007). CCT forms a hetero-oligomeric double-ring complex with eight subunits per ring (CCTα, β, γ, δ, ε, ζ, η, and θ in mammals) and functions as an ATP-dependent molecular chaperone required for correct folding of many cytosolic proteins, such as actin and tubulin (Yaffe *et al.*, 1992; Sternlicht *et al.*, 1993; Kubota *et al.*, 1994, 1995; Gutsche *et al.*, 1999; Llorca *et al.*, 1999, 2000; Dekker *et al.*, 2008). CCT is also known to prevent aggregation of polyglutamine (polyQ) proteins, which cause cytotoxicity and lead to neurodegenerative disorders, including Huntington's disease (Nollen *et al.*, 2004; Kitamura *et al.*, 2006). The *C. elegans* genome contains eight genes encoding the individual CCT subunits (*cct-1* to *cct-8*) (Leroux and Candido, 1995a,b, 1997; Matus *et al.*, 2010). These genes are ubiquitously expressed during all developmental stages and are essential for embryogenesis (Leroux and Candido, 1995a,b, 1997). In *C. elegans*, CCT is important for tubulin folding and microtubule growth in the early embryo (Srayko *et al.*, 2005; Lundin *et al.*, 2008). Although the function of CCT is known to be required for proper folding of actin and tubulin in yeast and cultured cells, its physiological roles in whole multicellular organisms remain elusive.

In this study, we sought to elucidate the mechanism(s) underlying the morphogenesis of epithelial cells. We found that a CCT-dependent actin supply is essential for the proper construction and maintenance of microvilli and the overall apical membrane structures in intestinal cells. These results demonstrate a physiological function of CCT in whole animals.

RESULTS

Chaperonin is required for normal apical morphology and intracellular trafficking in intestinal cells

To gain insight into how polarized epithelial cells are established and maintained, we searched for genes whose RNA interference (RNAi) knockdown affected either the localization of apical or basolateral marker proteins or the membrane morphology visualized by these markers. We chose P-glycoprotein-1 (PGP-1) and syntaxin-1

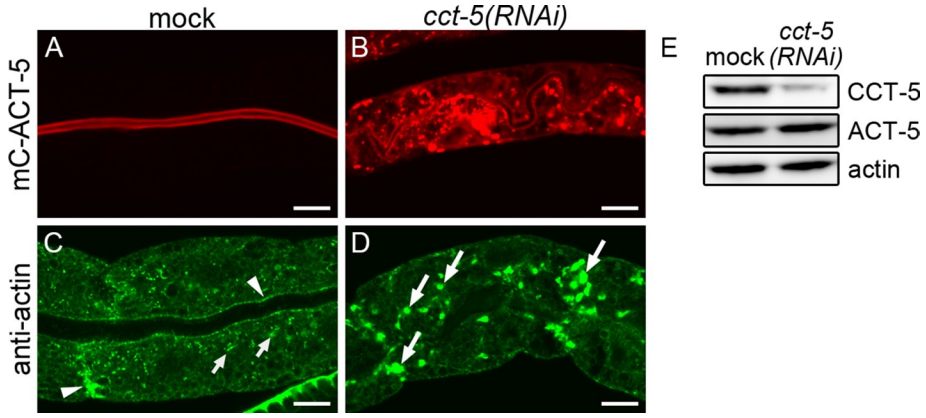

FIGURE 2: Depletion of CCT-5 causes aggregation of actin in intestinal cells. (A, B) Subcellular localizations of mCherry-ACT-5 (mC-ACT-5) in mock-treated or *cct-5(RNAi)* animals. The expression pattern of mC-ACT-5 in mock-treated animals is limited to the apical microvilli within the intestine (A). In *cct-5(RNAi)* animals, mC-ACT-5 forms large aggregates in the cytoplasm (B). The images show the results of L1 RNAi treatment. (C, D) Subcellular localizations of endogenous actin in intestinal cells. Endogenous actin is localized to the cortical region (arrowheads) and cytoplasmic structures (arrows) in the intestine of mock-treated animals (C). In the intestine of *cct-5(RNAi)* animals, many actin aggregates are observed in the cytoplasm (D, large arrows). (E) The actin protein levels are unaltered in *cct-5*–deficient animals. In C–E, L3 larvae were treated with RNAi for 3 d. Scale bars, 10 μm.

(SYN-1) as marker proteins of apical and basolateral membranes, respectively, and expressed these proteins with green fluorescent protein (GFP) tags (Figure 1, A and C; Sato *et al.*, 2011). We found that RNAi of *cct-5* encoding the ε-subunit of the CCT complex resulted in the formation of bubble-shaped aberrant membrane structures on the apical membrane of intestinal cells when L1 larvae were incubated on RNAi plates for 3 d (Figure 1B, inset, arrows). In such animals, GFP-PGP-1 was still mainly localized to the apical membrane, but a part of the protein also accumulated on cytoplasmic punctate structures (Figure 1B, arrowheads). When these animals were fed with Texas Red–dextran, it labeled the bubble-shaped aberrant membrane structures on the apical membrane, confirming that they were composed of deformed apical plasma membrane (Figure 1F). There were some GFP-PGP-1–positive cytoplasmic punctate structures that were not labeled with Texas Red–dextran (Figure 1G), suggesting that part of the GFP-PGP-1 was retained in intracellular compartments. The signals for Texas Red–dextran were restricted in the intestinal lumen and were not observed in the pseudocoelom of *cct-5(RNAi)* animals, suggesting that the barrier properties of the intestinal cells were maintained (Figure 1, F and G). On the other hand, GFP-SYN-1 was largely localized to the basolateral membrane in *cct-5(RNAi)* animals, although part of the GFP-SYN-1 was also detected on mesh-like structures near the lateral region and the cell periphery (Figure 1D). These results show that *cct-5(RNAi)* causes abnormal apical membrane structures and also partially affects the transport of apical and basolateral membrane proteins. Even in *cct-5(RNAi)* animals, we did not observe any mistargeting of GFP-PGP-1 or GFP-SYN-1 to the opposite plasma membrane domains (Figure 1, B and D). We further confirmed that the localizations of GFP-PGP-1 and mCherry-SYN-1 did not overlap even after *cct-5* RNAi (Supplemental Figure S1).

When *cct-5* RNAi was started at L1 larvae (L1 RNAi), the animals were arrested around the L3 larval stage. Meanwhile, L3 larvae treated with *cct-5* RNAi (L3 RNAi) reached adulthood. When L4 larvae were subjected to RNAi, *cct-5* RNAi induced a severe embryonic lethality or larval arrest phenotype in the F1 generation (Supplemental Figure S2C). Immunostaining using an anti–CCT-5 antibody showed that CCT existed diffusely in the cytoplasm but less in the nucleus, and the staining was abolished by *cct-5* RNAi (Supplemental Figure S2, A and B).

CCT depletion results in actin loss from microvilli and formation of actin aggregates in the cytoplasm

We examined whether loss of CCT function affected the biogenesis of ACT-5, the microvillus-specific actin, in intestinal cells, using mCherry-tagged ACT-5 (mC-ACT-5). Expression of mC-ACT-5 in *act-5(ok1397)*-knockout animals rescued the larval lethality, indicating that the fusion protein was functional (unpublished data). In mock-treated animals, mC-ACT-5 was specifically localized to the apical membrane of the intestinal cells (Figure 2A). When L1 or L3 larvae were treated with *cct-5* RNAi, mC-ACT-5 formed large aggregates in the cytoplasm in both cases (Figures 2B and 3E). We confirmed that the signal of these mC-ACT-5 aggregates was distinct from autofluorescence of gut granules (Supplemental Figure S3). Because RNAi knockdown of other CCT subunits resulted in similar phenotypes in terms of abnormal mC-ACT-5 localization (Supplemental Figure S2D), we mainly examine *cct-5* hereafter. Defects in the GFP-PGP-1 and mC-ACT-5 localizations were observed throughout the intestine of the *cct-5(RNAi)* animals (Supplemental Figure S2E). Immunostaining analysis of endogenous actin was conducted using a monoclonal anti–pan-actin antibody that recognized ubiquitously expressed actins but not ACT-5 (Figure 2, C and D). In the wild-type intestine, we observed strong staining of actin in the cortical region and in a number of cytosolic small puncta within intestinal cells but only weak staining of microvillar actin (Figure 2C), as reported previously (MacQueen *et al.*, 2005). In the *cct-5(RNAi)* animals, a large amount of endogenous actin accumulated in large aggregates (Figure 2D, large arrows). Such actin aggregates were also observed in the body wall muscles of the *cct-5(RNAi)* animals (Supplemental Figure S4B). The *cct-5(RNAi)* animals showed reduced thrashing movements when swimming in a buffer, suggesting defects in neuromuscular functions (Supplemental Figure S4C). We confirmed the efficiency of *cct-5* knockdown with an anti–CCT-5 antibody (Figure 2E). Using Western blotting, we detected CCT-5 as a single band of ~60 kDa in mock-treated animal lysates. The signal intensity of CCT-5 was greatly reduced after specific RNAi, confirming efficient knockdown and the specificity of the antibody. We also examined whether the actin protein levels were affected by the loss of CCT function (Figure 2E). RNAi of *cct-5* did not appear to affect the levels of ACT-5 or other actin molecules, indicating that the aggregates including actin were not efficiently removed from the cytoplasm.

We further investigated whether CCT disruption affected the level of F-actin in intestinal cells (Figure 3, A–I). In mock-treated animals, phalloidin was mainly observed in microvilli of the apical surface and colocalized with mC-ACT-5 (Figure 3, A–C). In *cct-5(RNAi)* animals, phalloidin signals were also observed in microvilli but to a lesser extent (Figure 3, D–I), and no colocalization with mC-ACT-5–positive aggregates was observed, indicating that the mC-ACT-5 aggregates contained very little F-actin. As a measure of molecular exchange, we subjected mC-ACT-5–labeled aggregates to fluorescence recovery

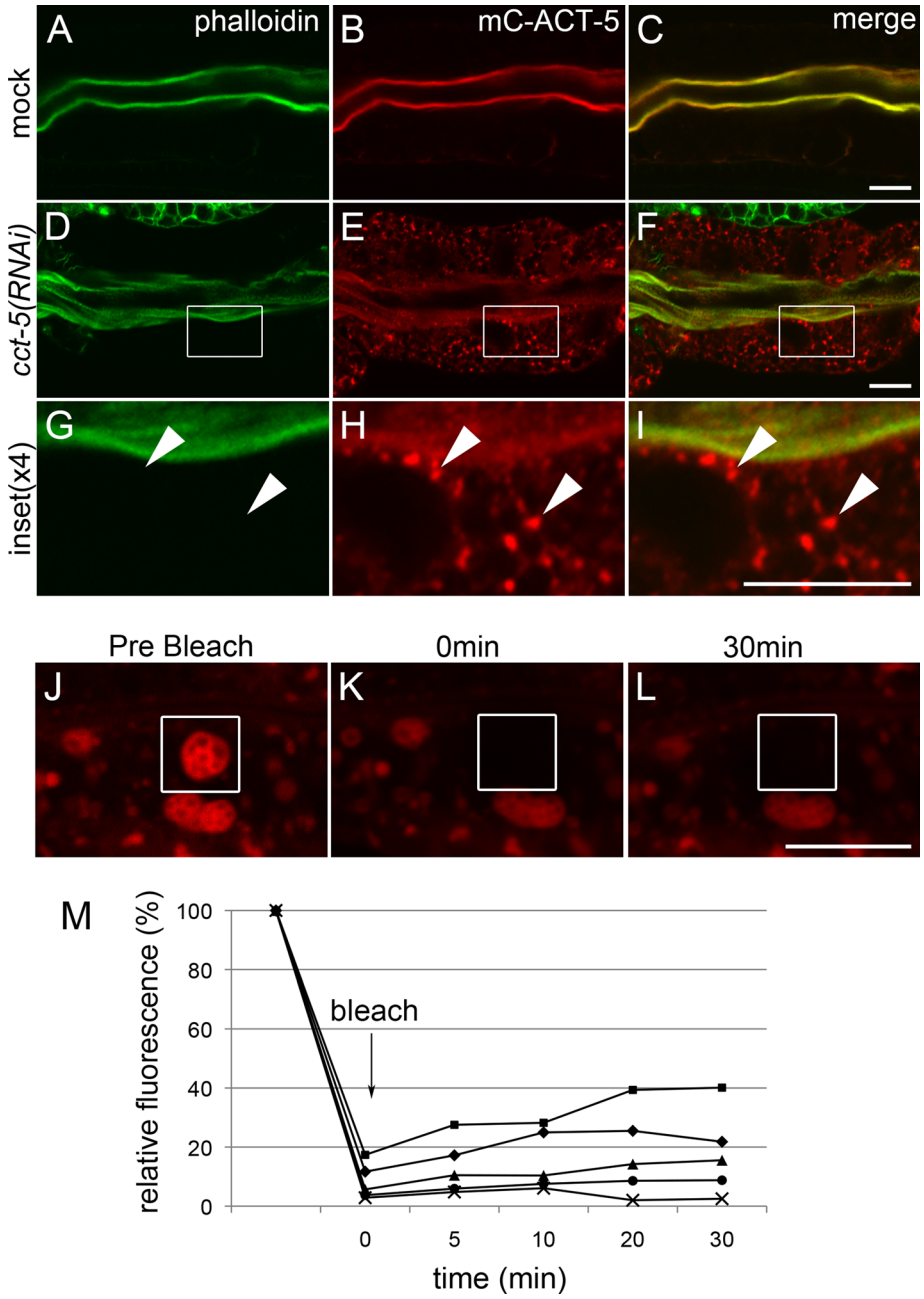

FIGURE 3: Actin forms aggregates in the absence of CCT function. (A–I) Actin aggregates in *cct-5*–deficient animals do not contain F-actin. Disruption of CCT function results in a reduced amount of F-actin in microvilli. Mock-treated and *cct-5(RNAi)* worms expressing mC-ACT-5 (B, E, H) were stained with phalloidin to visualize F-actin (A, D, G). Merged images are shown in C, F, and I. Enlarged (×4) images of the boxed areas in D–F are shown in G–I, respectively. Microvillus enrichment of F-actin is observed in mock-treated animals (A) and also in *cct-5(RNAi)* animals but to a lesser extent (D). The cytoplasmic actin aggregates in *cct-5(RNAi)* animals are not positive for phalloidin (G–I, arrowheads). Scale bars, 10 μm. (J–M) FRAP analysis of mC-ACT-5 on aggregated structures. Left to right: before photobleaching (Prebleach; J), immediately after bleaching (0 min; K), and 30 min after bleaching (L). The squares indicate the photobleached areas. For the graph, the fluorescence intensities in the squares were measured and provided as relative intensities based on the initial value before bleaching. Graphs indicate the results of five individual experiments (M). In these experiments, L3 larvae were treated with RNAi for 2 d.

after photobleaching (FRAP) analysis (Figure 3, J–M). The fluorescence recovery in individual aggregates was very slow, indicating that mC-ACT-5 associated with the aggregates was rarely exchanged with external pools.

Chaperonin is required for correct intestinal microvillus formation

To characterize the aberrant apical membrane structures in *cct-5(RNAi)* animals, we examined transgenic animals that expressed both GFP-PGP-1 and mC-ACT-5 in intestinal cells (Figure 4, A–I). We found that GFP-PGP-1 and mC-ACT-5 colocalized on the apical membrane in mock-treated animals (Figure 4, A–C). In *cct-5(RNAi)* animals, mC-ACT-5 colocalized with GFP-PGP-1 on the apical region with a smooth morphology but was absent in the bubble-like membrane structures, which were GFP-PGP-1 positive (Figure 4, D–I). Consistently, *act-5*-knockout animals expressing GFP-PGP-1 also displayed these bubble-like membrane structures of the apical surface (Figure 4, J–L). GFP-PGP-1 was largely localized on the apical membrane even in *act-5*-knockout animals, suggesting that the apicobasal polarity was maintained in the absence of the microvillar actin (Figure 4, J–L).

We further sought to define the defects in the intestines of CCT-deficient animals by electron microscopy. In the intestinal cells of wild-type animals, we observed a number of ordered, finger-like projections corresponding to microvilli anchored in the electron-dense terminal web underneath the apical membrane (Figure 5, A and C). Depletion of CCT functions resulted in a significant decrease in the length of the microvilli ($p < 0.01$), although the terminal web was still observed (Figure 5, B, D, and E). In *cct-5(RNAi)* animals, the interval of each microvillus appeared irregular, and the microvilli were sparse in some regions. These observations demonstrate that the CCT activity is required for normal organization of intestinal microvilli. In addition to the defects in microvilli, large vacuoles, electron-dense granules, and tubules were observed in the cytoplasm of the *cct-5(RNAi)* intestine. Undigested bacteria were often observed in the intestinal lumen of these animals, suggesting defects in food digestion and absorption (Figure 5, B and D).

Loss of CCT impairs tubulin biogenesis and microtubule formation

We further determined whether CCT depletion affected microtubules, using α-tubulin immunostaining (Figure 6, A–D). In mock-treated animals, α-tubulin was concentrated in the subapical region and on filamentous structures underneath the basal membrane (Figure 6, A and B). The antibody used also resulted in staining of a fine meshwork in the cytoplasm (Figure 6A). Depletion of CCT functions by L3 RNAi resulted in a reduction of the overall α-tubulin signals (Figure 6, C and D) and disorganization of the cytoplasmic microtubule structures (Figure 6C). The steady-state

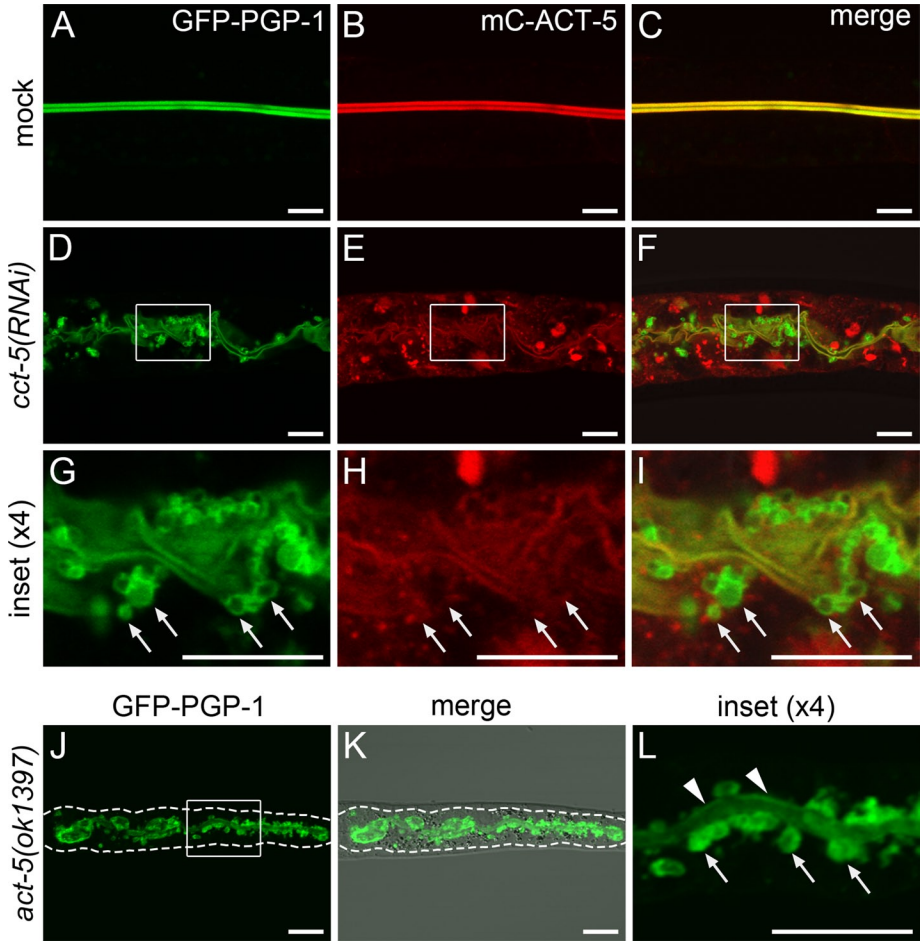

FIGURE 4: Abnormal apical membrane structures in CCT-deficient animals are caused by loss of ACT-5 from the microvilli. (A–I) The subcellular localizations of GFP-PGP-1 and mC-ACT-5 were observed in the intestines of mock-treated (A–C) or *cct-5(RNAi)* (D–I) animals. Depletion of CCT-5 results in less mC-ACT-5 in part of apical membrane, resulting in abnormal, bubble-like, GFP-PGP-1–positive structures (G–I, arrows). Merged images are shown in C, F, and I. Enlarged (×4) images of the boxed area in D–F are shown in G–I, respectively. Scale bars, 10 μm. The images show the results of L1 RNAi treatment. (J–L) Depletion of ACT-5 results in abnormal GFP-PGP-1–positive structures on the apical membrane. The subcellular localization of GFP-PGP-1 was observed in L1 larvae of the *act-5(ok1397)*-knockout animals. Note that GFP-PGP-1 is localized to the bubble-like membrane structures (arrows) connected to the apical membrane (arrowheads). Scale bars, 10 μm.

level of endogenous α-tubulin was reduced by ~70% (Figure 6E). These results show that CCT is required for proper tubulin biogenesis in vivo. We also directly examined the effect of tubulin deficiency on the apical membrane morphology. When *tba-2* was subjected to knockdown from the L1 larval stage, GFP-PGP-1 accumulated in cytoplasmic large punctate structures, indicating that microtubules were required for intracellular transport of GFP-PGP-1 during the larval stages (Figure 6, F and G). In addition, the severe loss of α-tubulin caused aggregation of mC-ACT-5, suggesting that the interplay between microtubules and actin microfilaments was required to maintain the integrity of polarized intestinal cells (Figure 6G). In contrast, when *tba-2* was subjected to knockdown from the L3 larval stage, the localizations of GFP-PGP-1 and mC-ACT-5 were hardly affected (Figure 6H). Under this condition, the total protein level of α-tubulin was markedly reduced (Figure 6I). These observations imply that tubulin is essential for actin localization and intracellular transport in growing larvae but to a lesser extent in adult animals. These findings also imply that the abnormal apical membrane structure caused by *cct-5* RNAi in adult animals is independent of tubulin deficiency.

In contrast to actin and tubulin, the loss of the CCT function did not strongly affect the localization and stability of intestine-specific intermediate filament IFB-2 (Figure 6, J and K). The *C. elegans* genome contains 11 genes encoding intermediate filaments, comprising a central α-helical rod domain and regularly spaced hydrophobic residues (Carberry *et al.*, 2009). Among these intermediate filaments, IFB-2 is expressed in the intestinal cells and is present in the electron-dense subapical layer of the terminal web and the junction-associated plaque materials (Bossinger *et al.*, 2004). In the mock-treated animals, IFB-2 was localized to the subapical region just beneath mC-ACT-5 (Figure 6J). The localization and amount of IFB-2 appeared unchanged in *cct-5(RNAi)* animals, although mC-ACT-5 formed aggregates in the cytosol (Figure 6K). The apical localization of ERM-1, a cytoskeletal linker protein of the ERM family required for epithelial integrity (van Fürden *et al.*, 2004), was not strongly affected in the *cct-5*–deficient intestinal cells under this RNAi condition (Supplemental Figure S5, A and B). The localization of the intestine filament organizer IFO-1 (Carberry *et al.*, 2012) was also unaffected in *cct-5(RNAi)* animals (Supplemental Figure S5, C and D). These results suggest that CCT acts more specifically on actin and tubulin in the intestinal cells.

DISCUSSION

In this study, we showed that CCT is important for the biogenesis of actin and tubulin in the intestines of intact whole organisms. In particular, we showed that CCT activity is essential for the formation and maintenance of microvilli in intestinal epithelial cells. Because the apical surface of intestinal epithelial cells is covered by microvillar protrusions, high levels of actin synthesis and folding activities are necessary in these cells. A CCT-dependent actin supply is also required to maintain the overall morphology of the apical surface. When CCT was subjected to knockdown, the subapical regions lacking actin localization were deformed and appeared as bubble-like structures.

In *C. elegans* intestinal cells, the loss of CCT function caused aggregation of actin and tubulin in the cytoplasm (Figures 2 and 6). However, the stability and localization of IFB-2 and ERM-1 appeared unaffected in *cct-5*–deficient cells under this condition, suggesting a substrate-specific function of CCT in vivo (Figure 6 and Supplemental Figure S5). Although CCT was originally believed to function specifically for actin and tubulin, recent studies revealed that it acts on more diverse substrates, comprising 9–15% of newly synthesized proteins in the range of 30–60 kDa (Thulasiraman *et al.*, 1999; Yam *et al.*, 2008). CCT can recognize a wide range of polypeptides, and CCT substrates share a number of similar properties. As an example, the CCT

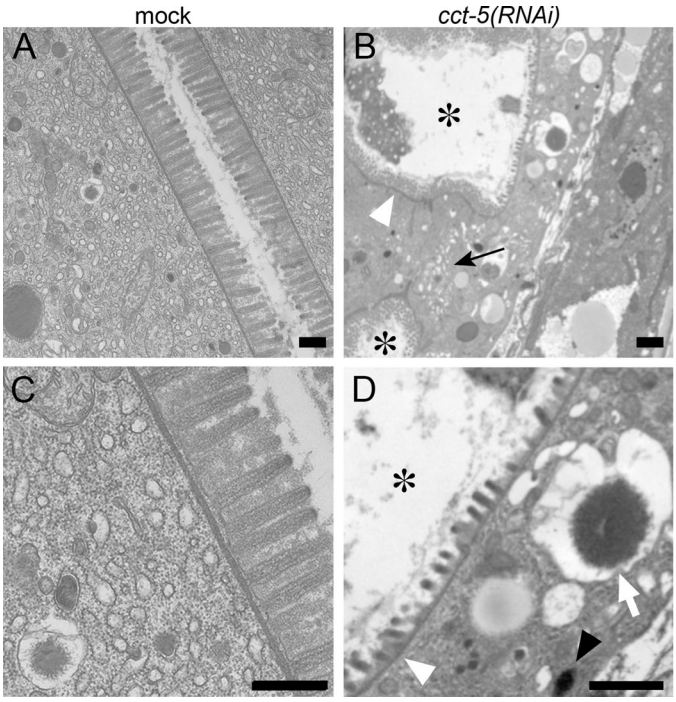

FIGURE 5: Electron microscopy analysis of wild-type and *cct-5(RNAi)* animals. (A–D) Electron micrographs of intestinal cross sections from wild-type and *cct-5(RNAi)* animals. (A, C) Mock-treated animals have a normal intestinal organelle distribution and highly ordered microvilli. The tubular network of the endoplasmic reticulum, vesicles, and granules are also observed. (B, D) In *cct-5(RNAi)* animals, the microvilli are reduced in size and sparse in some areas, although the terminal web is observed (white arrowheads). Two lumens are observed in a single section (asterisks in B and D). Electron-dense granules (black arrowhead in D), tubules (black arrow in B), and vacuoles (white arrow in D) are also observed in the cytoplasm. Undigested bacteria often accumulate in the gut lumen of *cct-5(RNAi)* animals. Scale bars, 1 μm. (E) Loss of CCT functions resulted in a significant decrease in the length of the microvilli. The lengths of the microvilli were quantified in mock and *cct-5 (RNAi)* animals and statically analyzed by Student's *t* test. Results are shown as a mean ± SD of the length of microvilli ($n = 147$ from three animals or $n = 182$ from five animals for mock or *cct-5 (RNAi)* animals, respectively). $^{**}p < 0.01$.

substrates Gβ-transducin (Kubota *et al.*, 2006) and CDC20 (Camasses *et al.*, 2003) share common motifs, such as the WD40 repeat. Various approaches demonstrated that many CCT substrates show a high β-sheet propensity and/or a low α-helical content, which is predicted to confer slow folding kinetics and make these proteins more prone to aggregation (Yam *et al.*, 2008). Given that IFB-2 has a long α-helical rod domain but neither a WD40 domain nor β-sheet propensity, it may not be an adequate substrate for CCT and could be folded by other chaperones such as HSP70, HSP90, and small heat shock proteins (Liang and MacRae, 1997). Such structural differences may account for the relatively moderate effects of CCT depletion on intermediate filament formation.

Although CCT activity is required for the folding of actin and tubulin molecules, the fates of unfolded actin and tubulin are different. The total levels of α-tubulin were obviously reduced in the *cct-5* mutant animals, suggesting that the unfolded tubulin molecules were degraded. In contrast, the protein levels of both cytosolic and microvillar actin were unchanged in the *cct-5*–deficient animals. Consistent with these observations, similar results have been reported in mammalian cultured cells (Grantham *et al.*, 2006). Unfolded actin formed large, stable aggregates in the cytoplasm that showed little exchange activity with external pools. These findings suggest that unfolded actin molecules tend to form aggregates that were not efficiently degraded. It has been reported that some mutations in cardiac α-actin, which cause hypertrophic or dilated cardiomyopathy, produce mutant proteins that are not efficiently folded by CCT (Vang *et al.*, 2005). Such mutant actin molecules are stable in the cytoplasm and can be recovered from the insoluble fraction using Triton X-100, suggesting that it is a general nature of unfolded actin molecules to form aggregates rather than undergo degradation (Vang *et al.*, 2005).

We showed that tubulin depletion during the larval stages causes severe defects in actin localization and GFP-PGP-1 transport. In contrast, when tubulin was subjected to knockdown from L3 larvae, its effect on actin organization and transport appeared relatively mild. These results suggest that the phenotypes observed in *cct-5* L3 RNAi animals were mostly dependent on actin deficiency rather than tubulin deficiency. To maintain microvillar structures, a continuous CCT-mediated actin supply appears to be essential. These observations also imply that tubulin is particularly important for microfilament organization and intracellular trafficking when cells are expanding their volume but to a lesser extent once cells have finished expansion in adulthood.

Mutations in the human CCT5 gene reportedly cause mutilating sensory neuropathy with spastic paraplegia, and mutations in the rat CCT4 gene cause heredity sensory neuropathy (Lee *et al.*, 2003; Bouhouche *et al.*, 2006). The requirements for CCT activity could be especially high in polarized cells such as neuronal and epithelial cells. Although the precise mechanisms of these diseases are not understood, one possibility is that the loss of correctly folded actin or tubulin in the absence of CCT function could disturb the integrity of the cytoskeleton, leading to neurodegeneration. Alternatively, the aggregates of CCT substrates, such as actin in the cytoplasm, could be cytotoxic to neuronal cells, as observed in polyQ diseases (Nollen *et al.*, 2004; Kitamura *et al.*, 2006). Further analyses using *C. elegans* would be useful to clarify the molecular mechanisms underlying chaperone-related diseases as well as the in vivo functions of CCT.

MATERIALS AND METHODS

C. elegans strains

Handling and culturing of *C. elegans* were conducted as described previously (Brenner, 1974). Strains expressing GFP- or mCherry-tagged proteins were grown at 20°C. The wild-type parent for all strains was *C. elegans* var Bristol strain N2. The *unc-119(ed3)* mutant (Maduro and Pilgrim, 1995) and VC971 (+/mT1 II; *act-5(ok1397)*/mT1[*dpy-10(e128)*] III) were obtained from the *Caenorhabditis* Genetic Center (University of Minnesota, Minneapolis, MN). The transgenic strains used were *dkIs259[Pact-5-GFP-pgp-1; unc-119(+)]*, *dkIs218[Popt-2-GFP-syn-1; Cb.unc-119(+)]* and *dkIs247[Pact-5-mCherry-HA-act-5; Cb.unc-119(+)]* (Sato *et al.*, 2011).

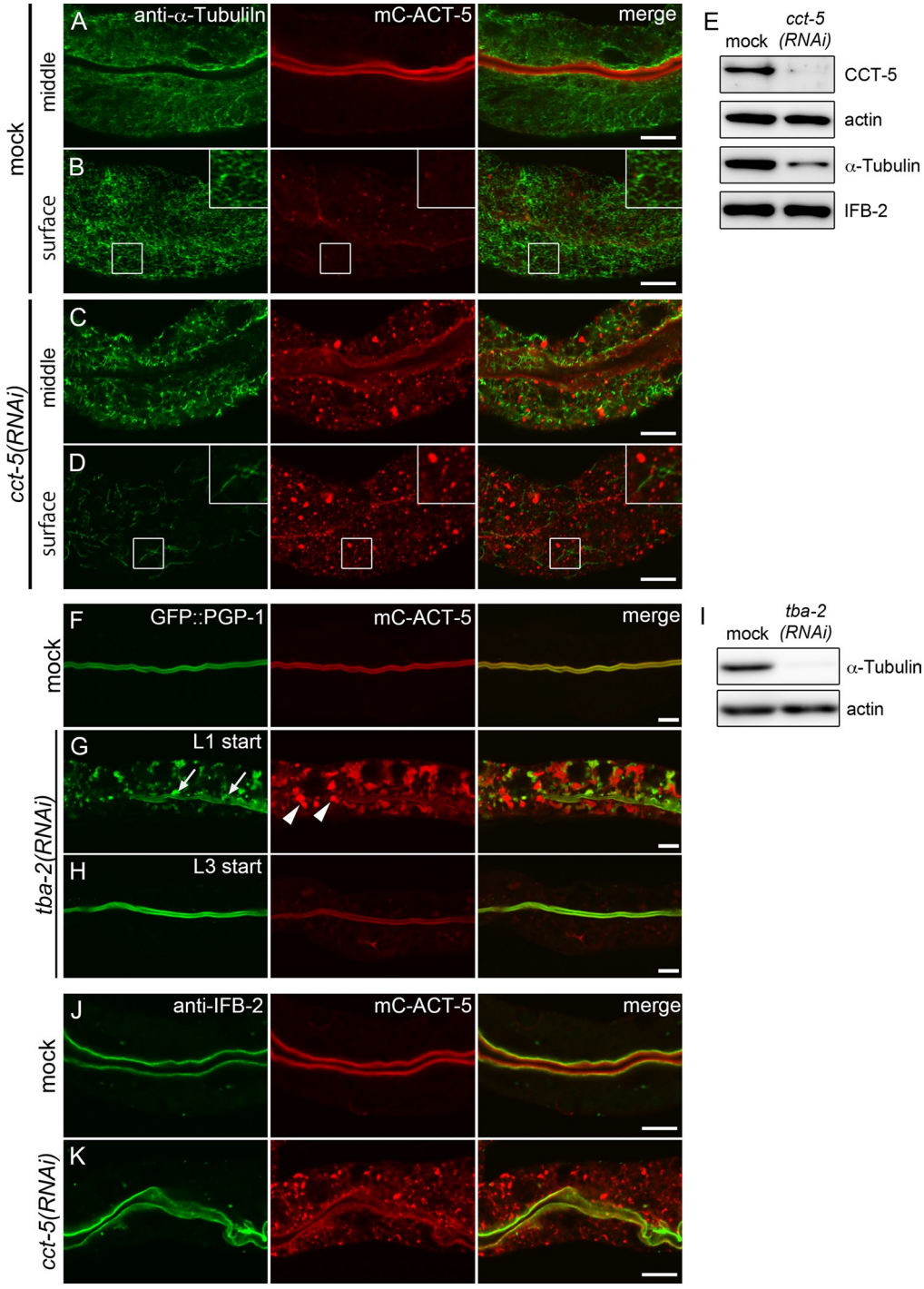

FIGURE 6: CCT is required for tubulin biogenesis and the formation of microtubules. (A–D) Animals expressing mC-ACT-5 were stained with an anti–α-tubulin antibody. In the intestines of mock-treated animals, the anti–α-tubulin antibody stains the cell cortex (A) and the tubular network underneath the plasma membrane (B). In *cct-5(RNAi)* animals, the tubulin signals in the cortex are reduced, and thicker and shorter microtubules are often observed near the plasma membrane (C, D). mC-ACT-5 and merged images are also shown. An enlarged (×2) image of the boxed area is shown in each inset (B, D). Scale bars, 10 μm. (E) Levels of actin, α-tubulin, and IFB-2 proteins in *cct-5(RNAi)* animals. In A–E, L3 larvae were subjected to RNAi for 2 d. (F–H) TBA-2, one of the α-tubulin proteins in *C. elegans*, was depleted by L1 or L3 RNAi in transgenic animals coexpressing GFP-PGP-1 and mC-ACT-5. L1 larvae were incubated for 3 d, and L3 larvae were incubated for 2 d on RNAi plates. The *tba-2* RNAi at L1 results in abnormal apical membrane structures (arrows) and mC-ACT-5 aggregation (arrowheads) (G). In contrast, *tba-2* RNAi from the L3 stage exhibits a normal GFP-PGP-1 localization and no aggregates of mC-ACT-5 (H). Scale bars, 10 μm. (I) Western blotting confirms that the total α-tubulin level is greatly reduced under the L3 RNAi condition. This result also suggests that *tba-2* RNAi is sufficient to reduce the total α-tubulin protein level, although *C. elegans* has multiple α-tubulin genes in the genome. (J, K) L3 animals expressing mC-ACT-5 were treated with RNAi for 2 d and stained with an anti-IFB-2 antibody. IFB-2 is detected in the apical cytocortex of intestinal cells from mock-treated (J) and *cct-5(RNAi)* (K) animals. mC-ACT-5 and merged images are also shown. Scale bars, 10 μm.

RNAi

We conducted RNAi experiments using a feeding method (Timmons *et al.*, 2001). L1 larvae were placed on nematode growth medium agar plates containing 5 mM isopropyl β-D-thiogalactopyranoside (IPTG) and *Escherichia coli* (strain HT115(DE3)) carrying double-stranded RNA expression constructs and allowed to grow at 20°C for 3 d. Otherwise, L3 larvae were incubated on RNAi plates at 20°C for 2 or 3 d and allowed to grow to the adult stage. The RNAi constructs fed to the animals contained a genomic DNA fragment of the *cct-5* gene, all other *cct* genes, or *tba-2* and were obtained from the Ahringer Genomic RNAi Library (Kamath and Ahringer, 2003). As a negative control, L4440 harboring a cDNA encoding the human transferrin receptor was used (Sato *et al.*, 2006).

Antibodies and Western blotting

We prepared a cDNA encoding *cct-5* from an EST clone (yk1389a05) provided by Yuji Kohara (National Institute of Genetics, Mishima, Japan) and cloned this into the pET24b expression vector (Invitrogen, Tokyo, Japan). A 6×histidine (His)-tagged recombinant protein was expressed in *E. coli* strain Rosetta (Merck, Tokyo, Japan) at 20°C for 8 h in the presence of 0.1 mM IPTG and purified using a Nickel Sepharose 6 Fast Flow column (GE Healthcare Biosciences, Uppsala, Sweden) under denaturing conditions according to the manufacturer's instructions. A keyhole limpet hemocyanin (KLH)–conjugated peptide selected from *C. elegans* ACT-5 (NH2-C+VAHDFESELAAA-COOH) as previously described (MacQueen *et al.*, 2005) was produced by Operon Biotechnologies (Tokyo, Japan). Purified proteins and peptides were used for antibody production in rabbits at TK Craft Corp. (Gunma, Japan). To examine the amounts of endogenous CCT-5 and ACT-5, total lysates were prepared from 50 adult hermaphrodites and subjected to Western blotting as described previously (Sato *et al.*, 2006). A monoclonal anti–pan-actin antibody (C4) was purchased from Millipore (Tokyo, Japan), and an anti-α-tubulin antibody (DM1a) was purchased from Sigma-Aldrich (Tokyo, Japan). Monoclonal anti–IFB-2 (MH33) and anti–ERM-1 (ERM1) antibodies developed by R. H. Waterston and M. L. Nonet, respectively, were obtained from the Developmental Studies Hybridoma Bank (University of Iowa, Iowa City, IA).

Construction of the strain expressing IFO-1–GFP

A destination vector, pPD117.01GtwyB(Asp718), was kindly provided by Barth D. Grant (Rutgers University, Piscataway, NJ) and contained a Gateway cassette B upstream of GFP. The *mec-7* promoter of pPD117.01GtwyB(Asp718) was replaced by the *act-5* promoter (pKS17). The cDNA fragment of *ifo-1* was cloned into pKS17 using Gateway recombination technology (Invitrogen). A transgenic line (*dkIs749[Pact-5-ifo-1-GFP; unc-119(+)]*) was created using the microparticle bombardment method as described previously (Praitis *et al.*, 2001). For a selection marker, the wild-type *unc-119* fragment was introduced simultaneously.

Immunostaining and microscopy

To observe live worms expressing transgenes, we mounted worms on agarose pads with 20 mM levamisole in M9 buffer (Sato *et al.*, 2008). Staining of dissected intestines was conducted as described previously (Grant and Hirsh, 1999; Sato *et al.*, 2006). Dissected intestines for α-tubulin, IFB-2, and ERM-1 staining were fixed in precooled (–20°C) methanol for 5 min. For pan-actin staining, dissected intestines were fixed in 3.7% formaldehyde/I-T solution (136 mM NaCl, 9 mM KCl, 1 mM $CaCl_2$, 3 mM $MgCl_2$, 77 mM glucose, 5 mM 4-(2-hydroxyethyl)-1-piperazineethanesulfonic acid [HEPES]–KOH, pH 7.4; Teramoto and Iwasaki, 2006) and fixed in precooled (–20°C) methanol for 5 min. For phalloidin staining, dissected intestines were fixed in 1 ml of fresh 1.25% paraformaldehyde/I-T solution at room temperature for 10 min. After fixation, the dissected intestines were washed four times in 1 ml of PTB buffer (1% bovine serum albumin [BSA], 1× phosphate-buffered saline [PBS], 0.1% Tween-20, 0.05% NaN_3, 1 mM EDTA) for 30 min at room temperature. The dissected intestines were then incubated with anti–pan-actin (C4; 1:1000 dilution), anti–α-tubulin (DM1a; 1:500), anti–IFB-2 (MH33; 1:100), and anti–ERM-1 (ERM1; 1:500) antibodies or Alexa Flour 488–phalloidin (1:1000) diluted in PTB buffer at 4°C overnight. After washing with PTC buffer (0.1% BSA, 1× PBS, 0.1% Tween-20, 0.05% NaN_3, 1 mM EDTA) four times, the samples were incubated with the appropriate secondary antibody conjugated to Alexa Fluor 488 (1:1000; Life Technologies Tokyo, Japan) at 4°C overnight. Whole-mount immunofluorescence staining of muscles was performed as described previously (Sato *et al.*, 2009). Images were obtained using an FV1000 or FV1200 confocal microscopy system (Olympus, Tokyo, Japan). Electron microscopy of *C. elegans* samples was conducted as described previously (Sato *et al.*, 2011).

Texas Red–dextran feeding assay

L1 larvae expressing GFP-PGP-1 were incubated on mock or *cct-5(RNAi)* plates at 20°C for 3 d. Approximately 30–40 worms were incubated in Egg buffer (118 mM NaCl, 48 mM KCl, 2 mM $CaCl_2$, 2 mM $MgCl_2$, 25 mM HEPES-NaOH, pH 7.3) containing 1 mg/ml Texas Red–dextran (40,000 molecular weight; Molecular Probes) for 90 min at 20°C. Worms were washed and mounted on agarose pads with 20 mM levamisole in Egg buffer. Images were obtained by using the FV1000 confocal microscopy system.

Fluorescence recovery after photobleaching analysis

The wide-field images of intestinal cells were obtained by using the FV1000 confocal microscopy system, and then the fluorescence of the small areas containing cytoplasmic mC-ACT-5 aggregates were photobleached by repeated scanning with the 543-nm laser at full power. After photobleaching, the time-lapse images of the wide-fields were further obtained for 30 min at 5-min intervals. The total fluorescence intensities in the photobleached areas were measured by using FV10-ASW (Olympus) and expressed as the relative fluorescence to the prebleach intensities.

ACKNOWLEDGMENTS

We thank Yuji Kohara and Barth D. Grant for supplying reagents. We thank the *Caenorhabditis* Genetic Center, which is funded by National Institutes of Health Office of Research Infrastructure Programs (P40 OD010440), for providing some strains. We also thank the Developmental Studies Hybridoma Bank (University of Iowa, Iowa City, IA), created by the National Institute of Child Health and Human Development of the National Institutes of Health, for providing monoclonal anti–IFB-2 and anti–ERM-1 antibodies. We thank the members of the Sato laboratory for technical assistance and discussions. K.S. was supported by the Funding Program for Next Generation World-leading Researchers (NEXT Program), the Sumitomo Foundation, The Mochida Memorial Foundation, and the Naito Foundation. M.S. was supported by a Grant-in-Aid for Young Scientists (A), Japan Society for the Promotion of Science; the Naito Foundation; the Cell Science Research Foundation; and the Uehara Memorial Foundation. This work was supported by the Joint Research Program of the Institute for Molecular and Cellular Regulation at Gunma University.

REFERENCES

Bossinger O, Fukushige T, Claeys M, Borgonie G, McGhee JD (2004). The apical disposition of the *Caenorhabditis elegans* intestinal terminal web is maintained by LET-413. Dev Biol 268, 448–456.

Bouhouche A, Benomar A, Bouslam N, Chkili T, Yahyaoui M (2006). Mutation in the epsilon subunit of the cytosolic chaperonin-containing t-complex peptide-1 (Cct5) gene causes autosomal recessive mutilating sensory neuropathy with spastic paraplegia. J Med Genet 43, 441–443.

Brenner S (1974). The genetics of *Caenorhabditis elegans*. Genetics 77, 71–94.

Camasses A, Bogdanova A, Shevchenko A, Zachariae W (2003). The CCT chaperonin promotes activation of the anaphase-promoting complex through the generation of functional Cdc20. Mol Cell 12, 87–100.

Carberry K, Wiesenfahrt T, Geisler F, Stocker S, Gerhardus H, Uberbach D, Davis W, Jorgensen E, Leube RE, Bossinger O (2012). The novel intestinal filament organizer IFO-1 contributes to epithelial integrity in concert with ERM-1 and DLG-1. Development 139, 1851–1862.

Carberry K, Wiesenfahrt T, Windoffer R, Bossinger O, Leube RE (2009). Intermediate filaments in *Caenorhabditis elegans*. Cell Motil Cytoskeleton 66, 852–864.

Dekker C, Stirling PC, McCormack EA, Filmore H, Paul A, Brost RL, Costanzo M, Boone C, Leroux MR, Willison KR (2008). The interaction network of the chaperonin CCT. EMBO J 27, 1827–1839.

Feldman JL, Priess JR (2012). A role for the centrosome and PAR-3 in the hand-off of MTOC function during epithelial polarization. Curr Biol 22, 575–582.

Gloerich M, ten Klooster JP, Vliem MJ, Koorman T, Zwartkruis FJ, Clevers H, Bos JL (2012). Rap2A links intestinal cell polarity to brush border formation. Nat Cell Biol 14, 793–801.

Gobel V, Barrett PL, Hall DH, Fleming JT (2004). Lumen morphogenesis in *C. elegans* requires the membrane-cytoskeleton linker erm-1. Dev Cell 6, 865–873.

Grant B, Hirsh D (1999). Receptor-mediated endocytosis in the *Caenorhabditis elegans* oocyte. Mol Biol Cell 10, 4311–4326.

Grantham J, Brackley KI, Willison KR (2006). Substantial CCT activity is required for cell cycle progression and cytoskeletal organization in mammalian cells. Exp Cell Res 312, 2309–2324.

Gutsche I, Essen LO, Baumeister W (1999). Group II chaperonins: new TRiC(k)s and turns of a protein folding machine. J Mol Biol 293, 295–312.

Horwich AL, Fenton WA, Chapman E, Farr GW (2007). Two families of chaperonin: physiology and mechanism. Annu Rev Cell Dev Biol 23, 115–145.

Hüsken K, Wiesenfahrt T, Abraham C, Windoffer R, Bossinger O, Leube RE (2008). Maintenance of the intestinal tube in *Caenorhabditis elegans*: the role of the intermediate filament protein IFC-2. Differentiation 76, 881–896.

Ikenouchi J, Hirata M, Yonemura S, Umeda M (2013). Sphingomyelin clustering is essential for the formation of microvilli. J Cell Sci 126, 3585–3592.

Kamath RS, Ahringer J (2003). Genome-wide RNAi screening in *Caenorhabditis elegans*. Methods 30, 313–321.

Karabinos A, Schunemann J, Weber K (2004). Most genes encoding cytoplasmic intermediate filament (IF) proteins of the nematode *Caenorhabditis elegans* are required in late embryogenesis. Eur J Cell Biol 83, 457–468.

Kitamura A, Kubota H, Pack CG, Matsumoto G, Hirayama S, Takahashi Y, Kimura H, Kinjo M, Morimoto RI, Nagata K (2006). Cytosolic chaperonin prevents polyglutamine toxicity with altering the aggregation state. Nat Cell Biol 8, 1163–1170.

Kubota H, Hynes G, Carne A, Ashworth A, Willison K (1994). Identification of six Tcp-1-related genes encoding divergent subunits of the TCP-1-containing chaperonin. Curr Biol 4, 89–99.

Kubota H, Hynes G, Willison K (1995). The eighth Cct gene, Cctq, encoding the q subunit of the cytosolic chaperonin containing TCP-1. Gene 154, 231–236.

Kubota S, Kubota H, Nagata K (2006). Cytosolic chaperonin protects folding intermediates of Gb from aggregation by recognizing hydrophobic b-strands. Proc Natl Acad Sci USA 103, 8360–8365.

Lee MJ, Stephenson DA, Groves MJ, Sweeney MG, Davis MB, An SF, Houlden H, Salih MA, Timmerman V, de Jonghe P, *et al.* (2003). Hereditary sensory neuropathy is caused by a mutation in the d subunit of the cytosolic chaperonin-containing t-complex peptide-1 (Cct4) gene. Hum Mol Genet 12, 1917–1925.

Leroux MR, Candido EP (1995a). Characterization of four new tcp-1-related *cct* genes from the nematode *Caenorhabditis elegans*. DNA Cell Biol 14, 951–960.

Leroux MR, Candido EP (1995b). Molecular analysis of *Caenorhabditis elegans tcp-1*, a gene encoding a chaperonin protein. Gene 156, 241–246.

Leroux MR, Candido EP (1997). Subunit characterization of the *Caenorhabditis elegans* chaperonin containing TCP-1 and expression pattern of the gene encoding CCT-1. Biochem Biophys Res Commun 241, 687–692.

Leung B, Hermann GJ, Priess JR (1999). Organogenesis of the *Caenorhabditis elegans* intestine. Dev Biol 216, 114–134.

Liang P, MacRae TH (1997). Molecular chaperones and the cytoskeleton. J Cell Sci 110, 1431–1440.

Llorca O, Martin-Benito J, Ritco-Vonsovici M, Grantham J, Hynes GM, Willison KR, Carrascosa JL, Valpuesta JM (2000). Eukaryotic chaperonin CCT stabilizes actin and tubulin folding intermediates in open quasi-native conformations. EMBO J 19, 5971–5979.

Llorca O, McCormack EA, Hynes G, Grantham J, Cordell J, Carrascosa JL, Willison KR, Fernandez JJ, Valpuesta JM (1999). Eukaryotic type II chaperonin CCT interacts with actin through specific subunits. Nature 402, 693–696.

Lundin VF, Srayko M, Hyman AA, Leroux MR (2008). Efficient chaperone-mediated tubulin biogenesis is essential for cell division and cell migration in *C. elegans*. Dev Biol 313, 320–334.

MacQueen AJ, Baggett JJ, Perumov N, Bauer RA, Januszewski T, Schriefer L, Waddle JA (2005). ACT-5 is an essential *Caenorhabditis elegans* actin required for intestinal microvilli formation. Mol Biol Cell 16, 3247–3259.

Maduro M, Pilgrim D (1995). Identification and cloning of *unc-119*, a gene expressed in the *Caenorhabditis elegans* nervous system. Genetics 141, 977–988.

Matus DQ, Li XY, Durbin S, Agarwal D, Chi Q, Weiss SJ, Sherwood DR (2010). *In vivo* identification of regulators of cell invasion across basement membranes. Sci Signal 3, ra35.

McGhee JD (2007). The *C. elegans* intestine. In: WormBook, ed. The *C. elegans* Research Community, WormBook, doi/10.1895/wormbook.1.133.1, www.wormbook.org.

McGhee JD, Fukushige T, Krause MW, Minnema SE, Goszczynski B, Gaudet J, Kohara Y, Bossinger O, Zhao Y, Khattra J, *et al.* (2009). ELT-2 is the predominant transcription factor controlling differentiation and function of the *C. elegans* intestine, from embryo to adult. Dev Biol 327, 551–565.

Nambiar R, McConnell RE, Tyska MJ (2010). Myosin motor function: the ins and outs of actin-based membrane protrusions. Cell Mol Life Sci 67, 1239–1254.

Nollen EA, Garcia SM, van Haaften G, Kim S, Chavez A, Morimoto RI, Plasterk RH (2004). Genome-wide RNA interference screen identifies previously undescribed regulators of polyglutamine aggregation. Proc Natl Acad Sci USA 101, 6403–6408.

Praitis V, Casey E, Collar D, Austin J (2001). Creation of low-copy integrated transgenic lines in *Caenorhabditis elegans*. Genetics 157, 1217–1226.

Rodriguez-Boulan E, Kreitzer G, Musch A (2005). Organization of vesicular trafficking in epithelia. Nat Rev Mol Cell Biol 6, 233–247.

Sato K, Ernstrom GG, Watanabe S, Weimer RM, Chen CH, Sato M, Siddiqui A, Jorgensen EM, Grant BD (2009). Differential requirements for clathrin in receptor-mediated endocytosis and maintenance of synaptic vesicle pools. Proc Natl Acad Sci USA 106, 1139–1144.

Sato M, Grant BD, Harada A, Sato K (2008). Rab11 is required for synchronous secretion of chondroitin proteoglycans after fertilization in *Caenorhabditis elegans*. J Cell Sci 121, 3177–3186.

Sato M, Saegusa K, Sato K, Hara T, Harada A, Sato K (2011). *Caenorhabditis elegans* SNAP-29 is required for organellar integrity of the endomembrane system and general exocytosis in intestinal epithelial cells. Mol Biol Cell 22, 2579–2587.

Sato K, Sato M, Audhya A, Oegema K, Schweinsberg P, Grant BD (2006). Dynamic regulation of caveolin-1 trafficking in the germ line and embryo of *Caenorhabditis elegans*. Mol Biol Cell 17, 3085–3094.

Segbert C, Johnson K, Theres C, van Furden D, Bossinger O (2004). Molecular and functional analysis of apical junction formation in the gut epithelium of *Caenorhabditis elegans*. Dev Biol 266, 17–26.

Srayko M, Kaya A, Stamford J, Hyman AA (2005). Identification and characterization of factors required for microtubule growth and nucleation in the early *C. elegans* embryo. Dev Cell 9, 223–236.

Sternlicht H, Farr GW, Sternlicht ML, Driscoll JK, Willison K, Yaffe MB (1993). The t-complex polypeptide 1 complex is a chaperonin for tubulin and actin *in vivo*. Proc Natl Acad Sci USA 90, 9422–9426.

Teramoto T, Iwasaki K (2006). Intestinal calcium waves coordinate a behavioral motor program in *C. elegans*. Cell Calcium 40, 319–327.

Thulasiraman V, Yang CF, Frydman J (1999). In vivo newly translated polypeptides are sequestered in a protected folding environment. EMBO J 18, 85–95.

Timmons L, Court DL, Fire A (2001). Ingestion of bacterially expressed dsRNAs can produce specific and potent genetic interference in *Caenorhabditis elegans*. Gene 263, 103–112.

van Fürden D, Johnson K, Segbert C, Bossinger O (2004). The *C. elegans* ezrin-radixin-moesin protein ERM-1 is necessary for apical junction remodelling and tubulogenesis in the intestine. Dev Biol 272, 262–276.

Vang S, Corydon TJ, Borglum AD, Scott MD, Frydman J, Mogensen J, Gregersen N, Bross P (2005). Actin mutations in hypertrophic and dilated cardiomyopathy cause inefficient protein folding and perturbed filament formation. FEBS J 272, 2037–2049.

Waterston RH, Hirsh D, Lane TR (1984). Dominant mutations affecting muscle structure in *Caenorhabditis elegans* that map near the actin gene cluster. J Mol Biol 180, 473–496.

Yaffe MB, Farr GW, Miklos D, Horwich AL, Sternlicht ML, Sternlicht H (1992). TCP1 complex is a molecular chaperone in tubulin biogenesis. Nature 358, 245–248.

Yam AY, Xia Y, Lin HT, Burlingame A, Gerstein M, Frydman J (2008). Defining the TRiC/CCT interactome links chaperonin function to stabilization of newly made proteins with complex topologies. Nat Struct Mol Biol 15, 1255–1262.